JOURNAL OF GUIDANCE, CONTROL, AND DYNAMICS
Vol. 16, No. 2, March–April 1993

Some Aspects of a Realistic Three-Dimensional Pursuit-Evasion Game

Fumiaki Imado*
Mitsubishi Electric Corporation, Hyogo 661, Japan

A three-dimensional pursuit-evasion game between a realistic missile and an aircraft is studied employing point-mass models for both vehicles. Since a direct method to solve this complicated mini-max problem is too time-consuming, the study is conducted by carrying out massive simulations in the parameter space of initial conditions and guidance law parameters. The important role of information in the opponent's acceleration to the game and the effectiveness of the strategy in rotating the line-of-sight vector are shown. It is found that there exist very few cases where the aircraft can avoid the missile, among them typical air-combat maneuvers such as linear acceleration, high-g barrel roll, split-S, and horizontal-S.

Nomenclature

$a_{c\max}$ = missile lateral acceleration command limit
a_{mp}, a_{my} = missile acceleration components measured in aircraft pitch and yaw axis, respectively
a_p, a_y, a_{pc}, a_{yc} = missile-pitch and yaw-axis lateral accelerations and their command signals
a_{pt}, a_{yt} = aircraft-desired pitch and yaw acceleration components, respectively
a_{tp}, a_{ty} = aircraft acceleration components measured in missile pitch and yaw axis, respectively
C_D = drag coefficient
C_{D0} = zero-lift drag coefficient
$C_L, C_{L\alpha}$ = lift coefficient and lift coefficient derivative
D, D_m = aircraft and missile drag, respectively
g = acceleration of gravity
g_{bias} = gravity compensation term in missile guidance system
h = altitude
k = aircraft-induced drag coefficient
k_1, k_2 = missile drag coefficients
L = lift
M = Mach number
MD = miss distance
m = mass
N_e, N_{e_t} = missile and aircraft effective navigation constants, respectively
r, r_x, r_y, r_z = relative range between missile and aircraft and its inertial x, y, and z components, respectively
s = reference area
T = thrust
t = time
v = velocity
v_c = closing velocity
x, y, z = inertial coordinates
α, α_0 = angle of attack and zero lift angle
γ, ψ = flight path and azimuth angles, respectively
η = introduced angle to rotate line-of-sight vector
ρ = air density
$\bar{\sigma}, \dot{\sigma}_p, \dot{\sigma}_y$ = line-of-sight rate vector and its pitch and yaw components, respectively
$\dot{\sigma}_{xI}, \dot{\sigma}_{yI}, \dot{\sigma}_{zI}$ = inertial x, y, and z components of $\bar{\sigma}$, respectively
τ = missile time constant
τ_α, τ_ϕ = aircraft α and ϕ control time constants, respectively
ϕ = aircraft roll angle
$(\dot{})$ = time derivative
$(\bar{})$ = vector

Subscripts

0 = initial value
c = control command signal
f = terminal (final) value
I = inertial coordinate
max = maximum value
min = minimum value
m = missile
p = pitch component
t = aircraft (target)
y = yaw or y component

Introduction

PURSUIT-EVASION problems between two vehicles have attracted considerable interest in recent years and many studies have appeared in the literature. However, their results still seem to be difficult to apply to actual air combat. That is, most studies have been devoted to obtaining precise solutions for very simplified problems. Recently, some studies[1,2] have dealt with a rather complicated practical model, but solved only a few specific cases.

The early studies of Isaacs[3] and Merz[4] showed the existence of a large number of different kinds of solutions for a very simple problem called the "homicidal chauffeur." Actually, an enormous number of solutions may exist for multidimensional nonlinear differential games with practical significance; it is simply impossible to know all the different kinds of solutions. It may be more helpful to pilots to find some features of the solutions where missile avoidance is successful, even if they are not precisely solved by a differential game approach.

This paper studies the pursuit-evasion problem between a missile and an aircraft. The missile is assumed to employ PNG (proportional navigation guidance) or APNG[5] (augmented PNG), each of which is obtained as the optimal control against a nonmaneuvering and a maneuvering target. Basically, these guidance laws try to nullify the LOS (line-of-sight) change. The aircraft is assumed to employ the same LOS information that the missile employs in PNG and APNG, but uses it to avoid the missile by rotating the LOS relative to the missile. By maneuvering the aircraft in an arbitrary direction normal to the LOS vector, the game changes from a "semidifferen-

Received July 14, 1990; revision received Feb. 15, 1992; accepted for publication Feb. 29, 1992.

*Chief Engineer, Advanced Mechanical Systems Department, Central Research Laboratory, Tsukaguchi Amagasaki. Member AIAA.

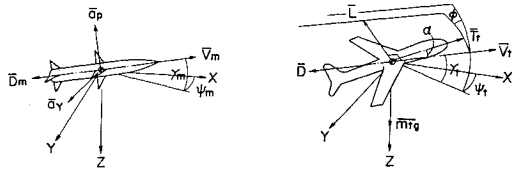

Fig. 1 Missile and aircraft symbols.

tial game'' to ''semicooperative interception.'' Simulations are conducted for a combination of guidance laws, PNG and APNG as employed by both vehicles, and for a set of various parameters such as initial relative geometries, navigation constants, and the aircraft initial evasive direction.

In this paper, the mathematical models of the dynamics and the guidance laws of the missile and aircraft are explained first. Second, the results of the simulation study are summarized. Third, some features of typical solutions are illustrated and discussed.

Mathematical Simulation Model

Figure 1 shows missile and aircraft symbols. Point-mass models are used for both vehicles, and a no side-slip condition is assumed for the aircraft (i.e., the side-slip angle is always reduced to 0 deg by rudder control). The equations employed are as follows.

Aircraft Dynamics

$$\dot{v}_t = \frac{1}{m_t}(T_t \cos\alpha - D) - g \sin\gamma_t \tag{1}$$

$$\dot{\gamma}_t = \frac{1}{m_t v_t}(L + T_t \sin\alpha)\cos\phi - \frac{g}{v_t}\cos\gamma_t \tag{2}$$

$$\dot{\psi}_t = \frac{(L + T_t \sin\alpha)}{m_t v_t \cos\gamma_t}\sin\phi \tag{3}$$

$$\dot{x}_t = v_t \cos\gamma_t \cos\psi_t \tag{4}$$

$$\dot{y}_t = v_t \cos\gamma_t \sin\psi_t \tag{5}$$

$$\dot{h}_t = v_t \sin\gamma_t \tag{6}$$

where

$$L = \tfrac{1}{2}\rho v_t^2 s_t C_L \tag{7}$$

$$C_L = C_{L\alpha}(\alpha - \alpha_0) \tag{8}$$

$$D = \tfrac{1}{2}\rho v_t^2 s_t C_D \tag{9}$$

$$C_D = C_{D0} + kC_L^2 \tag{10}$$

Missile Dynamics

$$\dot{v}_m = \frac{1}{m_m}(T_m - D_m) - g \sin\gamma_m \tag{11}$$

$$\dot{a}_p = (a_{pc} - a_p)/\tau \tag{12}$$

$$\dot{a}_y = (a_{yc} - a_y)/\tau \tag{13}$$

$$\dot{\gamma}_m = (a_p - g\cos\gamma_m)/v_m \tag{14}$$

$$\dot{\psi}_m = \frac{a_y}{v_m \cos\gamma_m} \tag{15}$$

$$\dot{x}_m = v_m \cos\gamma_m \cos\psi_m \tag{16}$$

$$\dot{y}_m = v_m \cos\gamma_m \sin\psi_m \tag{17}$$

$$\dot{h}_m = v_m \sin\gamma_m \tag{18}$$

where

$$D_m = k_1 v_m^2 + k_2 \frac{a_p^2 + a_y^2}{v_m^2} \tag{19}$$

Missile Control

Proportional Navigational Guidance

Roll-stabilized proportional navigation is assumed with signal saturation taken into account. The pitch and yaw-axis acceleration commands a_{pc} and a_{yc} are given by

$$a_{pc} = \begin{cases} N_e v_c \dot{\sigma}_p + g_{\text{bias}} & \text{for } |a_{pc}| \le a_{c\max} \\ a_{c\max}\,\text{sign}(a_{pc}) & \text{for } |a_{pc}| > a_{c\max} \end{cases} \tag{20}$$

and

$$a_{yc} = \begin{cases} N_e v_c \dot{\sigma}_y & \text{for } |a_{yc}| \le a_{c\max} \\ a_{c\max}\,\text{sign}(a_{yc}) & \text{for } |a_{yc}| > a_{c\max} \end{cases} \tag{21}$$

where g_{bias} is the compensation term for gravity and is given by

$$g_{\text{bias}} = g \cos\gamma_m \tag{22}$$

In Eqs. (20) and (21), N_e is the effective navigation constant, $\dot{\sigma}_p$ and $\dot{\sigma}_y$ are the target LOS rate vector pitch and yaw components measured in the missile body axes, and v_c is the closing velocity given by

$$\bar{\dot{\sigma}} = \frac{\bar{r}\times(\mathrm{d}/\mathrm{d}t)\bar{r}}{\bar{r}\cdot\bar{r}} = \frac{1}{r^2}\begin{bmatrix} r_y\dot{r}_z - r_z\dot{r}_y \\ r_z\dot{r}_x - r_x\dot{r}_z \\ r_x\dot{r}_y - r_y\dot{r}_x \end{bmatrix} = \begin{bmatrix} \dot{\sigma}_{xI} \\ \dot{\sigma}_{yI} \\ \dot{\sigma}_{zI} \end{bmatrix}_I \tag{23}$$

$$\dot{\sigma}_p = -\sin\psi_m \dot{\sigma}_{xI} + \cos\psi_m \dot{\sigma}_{yI} \tag{24}$$

$$\dot{\sigma}_y = \sin\gamma_m(\cos\psi_m \dot{\sigma}_{xI} + \sin\psi_m \dot{\sigma}_{yI}) + \cos\gamma_m \dot{\sigma}_{zI} \tag{25}$$

and

$$v_c = -\dot{r} = \frac{-(r_x\dot{r}_x + r_y\dot{r}_y + r_z\dot{r}_z)}{r} \tag{26}$$

where r is the missile-aircraft relative range and r_x, r_y, and r_z are its inertial three-axes components.

Augmented Proportional Navigation Guidance

APNG is introduced to approximate the game as a perfect information differential game. In APNG, the target (aircraft) acceleration must be employed. Practically, this value must be estimated under a noisy condition, and the use of an extended Kalman filter[6] is assumed here. Figure 2 shows an example of the estimated target acceleration. Simulation results of the APNG employing this estimated acceleration showed good improvement over ordinary PNG, but here mathematically calculated exact acceleration is used, as shown in later sections. The reason is to avoid the introduction of subsidiary effects on the game caused by noise. Once the target acceleration components a_{tp} and a_{ty}, measured in the missile pitch and yaw axes, are obtained, the pitch and yaw acceleration commands a_{pc} and a_{yc}, with APNG, are given by

$$a_{pc} = \begin{cases} N_e(v_c\dot{\sigma}_p + \tfrac{1}{2}a_{tp}) + g_{\text{bias}} & \text{for } |a_{pc}| \le a_{c\max} \\ a_{c\max}\,\text{sign}(a_{pc}) & \text{for } |a_{pc}| > a_{c\max} \end{cases} \tag{27}$$

and

$$a_{yc} = \begin{cases} N_e(v_c\dot{\sigma}_y + \tfrac{1}{2}a_{ty}) & \text{for } |a_{yc}| \le a_{c\max} \\ a_{c\max}\,\text{sign}(a_{yc}) & \text{for } |a_{yc}| > a_{c\max} \end{cases} \tag{28}$$

where

$$a_{tp} = -\sin\gamma_m(\cos\psi_m\ddot{x}_t + \sin\psi_m\ddot{y}_t) - \cos\psi_m\ddot{z}_t \quad (29)$$

$$a_{ty} = -\sin\gamma_m\ddot{x}_t + \cos\gamma_m\ddot{y}_t \quad (30)$$

Aircraft Control

PNG-Based Strategy

The LOS rate vector from the aircraft to the missile is obtained by changing the sign of $\bar{r}$ in Eq. (23), which results in the same equation as (23). The pitch and yaw components of $\bar{\sigma}$: $\dot{\sigma}_{pt}$ and $\dot{\sigma}_{yt}$ measured in the aircraft body axes are given by

$$\dot{\sigma}_{pt} = -\sin\psi_t\dot{\sigma}_{xI} + \cos\psi_t\dot{\sigma}_{yI} \quad (31)$$

and

$$\dot{\sigma}_{yt} = \sin\gamma_t(\cos\psi_t\dot{\sigma}_{xI} + \sin\psi_t\dot{\sigma}_{yI}) + \cos\gamma_t\dot{\sigma}_{zI} \quad (32)$$

Analogous to the missile PNG, the aircraft has to produce the acceleration components a_{p0} and a_{y0} in the pitch and yaw directions, but for evasion purposes, those signs should be reversed.

$$a_{p0} = -N_{et}v_c\dot{\sigma}_{pt} \quad (33)$$

$$a_{y0} = -N_{et}v_c\dot{\sigma}_{yt} \quad (34)$$

Our previous studies showed that the high-g barrel roll[9] is quite an efficient evasive maneuver against PNG and APNG missiles; the prominent feature of the maneuver is producing LOS rate change by rotating the LOS vector in a pitch-yaw plane. Motivated by this fact, the arbitrary angle η, shown in Fig. 3, is introduced to rotate the LOS vector. Then, the desired pitch and yaw acceleration components of the aircraft are

$$a_{pt} = a_{p0}\cos\eta + a_{y0}\sin\eta \quad (35)$$

and

$$a_{yt} = -a_{p0}\sin\eta + a_{y0}\cos\eta \quad (36)$$

When $\eta = 0$, the game becomes a semidifferential game, where the missile pursues by PNG or APNG, while the aircraft

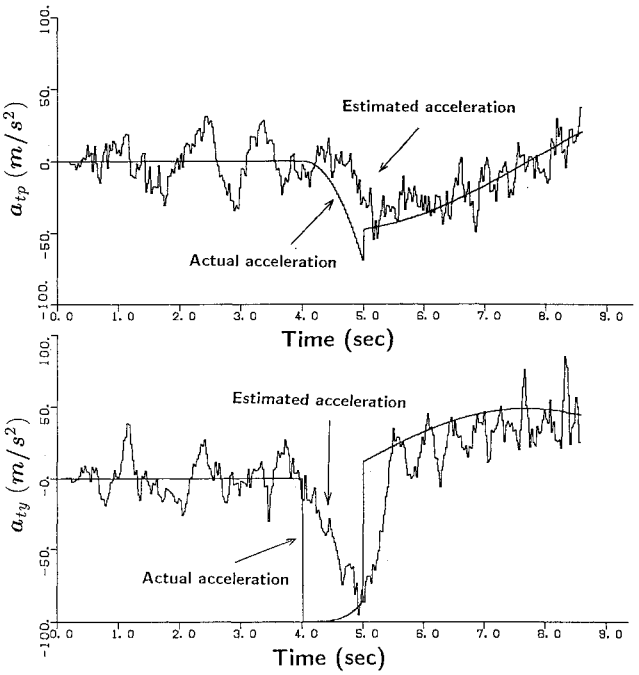

Fig. 2 Estimation example by extended Kalman filter (sampling time = 30 ms).

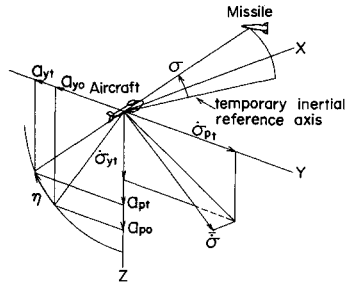

Fig. 3 LOS, its rate vector, and η employed in aircraft control.

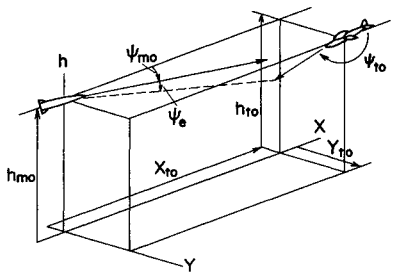

Fig. 4 Initial relative geometry.

evades capture by a strategy contrary to that of the missile. With $\eta = \pm 180$ deg, the game becomes a semicooperative interception, and with $\eta = \pm 90$ deg, the aircraft evades the missile by rotating the LOS vector normal to the current maneuvering plane. In order to obtain the desired aircraft acceleration, the aircraft α and ϕ are determined as follows:

$$(L + T_t\sin\alpha)\sin\phi = m_t a_{yt} \quad (37)$$

$$(L + T_t\sin\alpha)\cos\phi - m_t g\cos\gamma_t = m_t a_{pt} \quad (38)$$

By approximating $\sin\alpha \cong \alpha$ and from the foregoing equations, we obtain

$$\phi = \tan^{-1}\left[a_{yt}/(a_{pt} + g\cos\gamma_t)\right] \quad (39)$$

and

$$\alpha = m_t\left[(a_{pt} + g\cos\gamma_t)^2 + a_{yt}^2\right]^{1/2}/(\tfrac{1}{2}\rho v_t^2 s_t C_{L\alpha} + T_t) \quad (40)$$

APNG-Based Strategy

Analogous to the missile APNG, a_{p0} and a_{y0} in (33) and (34) are modified as

$$a_{p0} = -N_{et}(v_c\dot{\sigma}_{pt} + \tfrac{1}{2}a_{mp}) \quad (41)$$

and

$$a_{y0} = -N_{et}(v_c + \tfrac{1}{2}a_{my}) \quad (42)$$

where a_{mp} and a_{my} are the missile acceleration components measured in the aircraft body axes and are expressed by

$$a_{mp} = -\sin\gamma_t(\cos\psi_t\ddot{x}_m + \sin\psi_t\ddot{y}_m) - \cos\gamma_t\ddot{z}_m \quad (43)$$

and

$$a_{my} = -\sin\gamma_t\ddot{x}_m + \cos\gamma_t\ddot{y}_m \quad (44)$$

Simulation Conditions

Only a few initial relative geometries are selected in this study. The reader should note that the strategy of the aircraft

will change greatly according to the relative range to a missile, altitude, and initial aspect, etc. However, many informative results appear in this limited study. Figure 4 shows the initial geometry of a missile and an aircraft. A set of nominal parameters for both vehicles are given in Table 1. The initial altitude of the vehicles is set at 3000 m; the modeled aircraft can produce a maximum normal acceleration of 7 g's at this altitude. Under a high-g condition, it becomes rather difficult to maneuver an aircraft with a large roll rate; therefore, the maximum roll rate command $\dot{\phi}_{c\max}$ is treated as a function of α.

Simulations are conducted for a combination of missile guidance law, PNG or APNG, and that of the aircraft, PNG- or APNG-based. As for the latter, the determined strategy is to rotate the relative LOS vector, and the arbitrary rotation angle η is changed over the -180 to 180 deg range. The effective navigation constant of the missile N_e is set to 3 or 4; that of the aircraft N_{e_t} is set to 4 or 6. In the simulations, the aircraft is given a command in the first second to take the maximum angle of attack and a preset roll angle. After that, the aircraft evasive control algorithm stated in the preceding section is activated. This initial ϕ command is changed from -180 to 180 deg at intervals of 45 deg.

Table 1 Nominal parameters

Aircraft	
m_t	= 7500 kg
S_t	= 26.0 m^2
v_{t0}	= 290 m/s
h_{t0}	= 3000 m
x_{t0}	= 4000 m
$C_{L\alpha}$	= 4.01/rad
C_{D0}	= 0.0169
k	= 0.179
$\alpha_{\max}$	= 0.13 rad
T_t	= 65,000 N
τ_α	= 0.3 s
τ_ϕ	= 0.2 s
$\dot{\phi}_{c\max}$	= 16 rad/s ($\alpha = 0$)
	= 8 rad/s ($\alpha = 0.065$ rad)
	= 3.2 rad/s ($\alpha = 0.13$ rad)
Missile	
m_m	= 150 kg (coasting)
v_{m0}	= 600 m/s
h_{m0}	= 3000 m
x_{m0}	= 0 m
$C_{L\alpha}$	= 35.0/rad (at 2 M)
C_{D0}	= 0.74 (at 2 M)
k	= 0.03 (at 2 M)
T_m	= 0 (coasting)
$a_{c\max}$	= 30 g
τ	= 0.3 s
With sustainer	
m_m	= 165 kg ($t = 0$), 150 kg ($t = 6$ s)
T_m	= 5880 N ($0 \le t \le 6$ s)

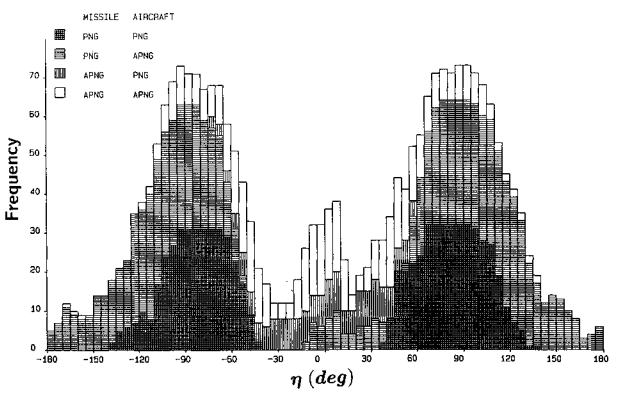

Fig. 5 Frequency (MD > 5 m) in relation to η.

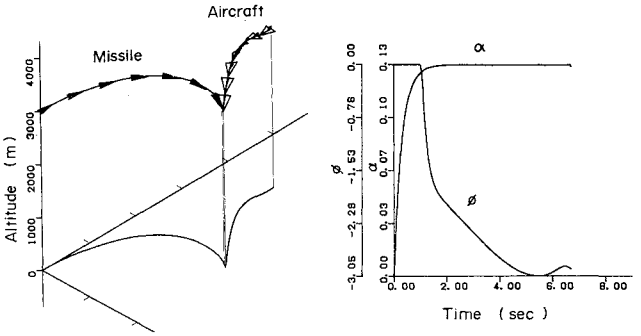

Fig. 6 Split-S, PNG ($N_e = 3$) vs PNG-based ($N_{e_t} = 4$) $y_{t0} = 1000$ m, $\psi_e = 0.363$, $\eta = 0.70$, $\phi_{c0} = 0$, MD = 30.4 m.

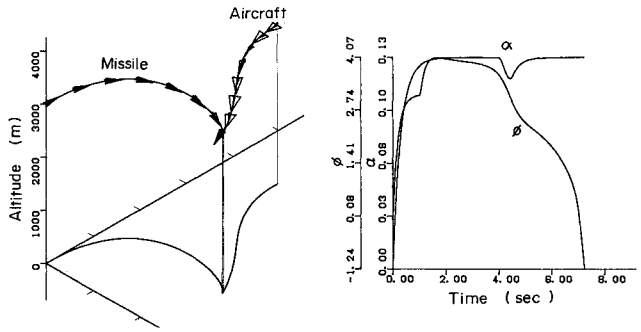

Fig. 7 Horizontal-S, PNG ($N_e = 3$) vs APNG-based ($N_{e_t} = 4$) y_{t0} = 1000 m, $\psi_e = 0.363$, $\eta = 0.26$, $\phi_{c0} = 3.14$, MD = 48.5 m.

Some Features of the Results

For a specified initial condition, with the combination of guidance laws, navigation constants η, and initial ϕ_c, typically 9216 simulations are conducted on a CRAY YMP. When symmetry exists in the vertical plane, the number is reduced by half. Figure 5 shows a typical example of the frequency of large miss distance in relation to the guidance law combination and η. The ordinate shows the number of cases where miss distance becomes greater than 5 m, among 128 cases in each η. In PNG missile vs PNG aircraft cases, large MDs (miss distances) are mainly produced near $\eta = \pm 90$ deg. In APNG missile vs PNG aircraft cases, the numbers are very small and only appear near $\eta = 0$ deg. APNG aircraft generally produce larger MDs than PNG aircraft; therefore, they have a greater chance of avoiding missiles. It seems strange that large MDs exist near $\eta = \pm 180$ deg, where both vehicles are supposed to cooperate to intercept each other. Since PNG and APNG are optimal guidance laws against maneuvering and nonmaneuvering targets, respectively, when both vehicles take the guidance laws separately, there is competition between both vehicles' controls, which is what produces large MDs. The following are some effects of other parameters.

In the early stage of the study, it was found that the aircraft navigation constant N_{e_t} should be larger than that of the missile N_e if the aircraft is to avoid the missile. In relation to the aircraft g performance and response speed, larger values of v_{t0}, $\alpha_{\max}$, T_t, and $\dot{\phi}_{c\max}$ increase the MD, whereas larger time constants τ_α and τ_ϕ decrease it. The former three parameters, v_{t0}, $\alpha_{\max}$ and T_t greatly effect the MD, whereas the effects of the latter three parameters, $\phi_{c\max}$, τ_α, and τ_ϕ, are relatively small. On the contrary, the larger values of the missile parameters v_{m0}, T_m, and $a_{c\max}$ greatly decrease the MD, and the smaller time constant τ decreases it. At the adopted initial condition, the missile initial heading error ψ_e is supposed to be eliminated, but the case may still exist where ψ_e remains for a lock-on-after-launch-type missile. Although the effect of ψ_e on miss distance is generally large, it depends on the air-

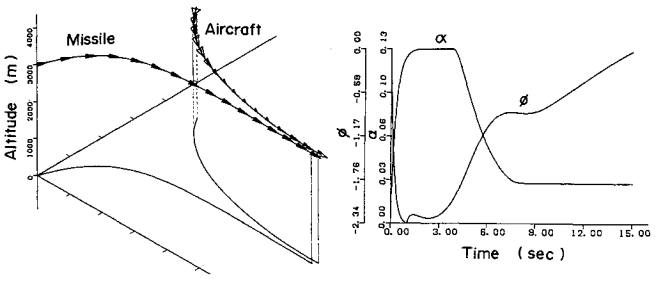

Fig. 8 Linear acceleration, PNG ($N_e = 3$) vs PNG-based ($N_{e_t} = 4$) $y_{t0} = 1000$ m, $\psi_e = 0$, $\psi_{m0} = 0.363$, $\eta = 0.52$, $\phi_{c0} = -2.36$, MD = 141.6 m.

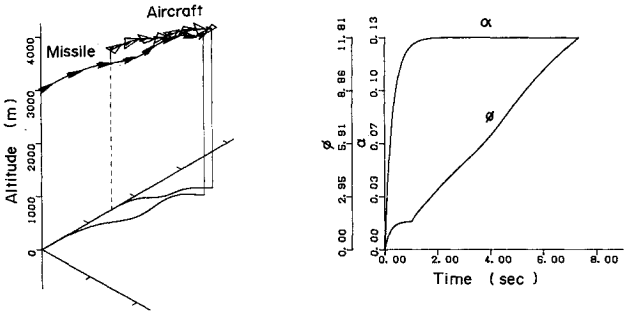

Fig. 9 High-g barrel roll, APNG ($N_e = 4$) vs APNG-based ($N_{e_t} = 4$) $x_{t0} = 1500$ m, $y_{t0} = 0$ m, $\psi_e = 0$, $\eta = -0.61$, $\phi_{c0} = 1.57$, MD = 191.0 m.

craft's initial ϕ_c. That is, in cases where the initial ϕ_c tends to eliminate ψ_e, the MD becomes smaller than cases without ψ_e. In most cases, the MD becomes very small; however, a small number of cases remain (typically less than 1%) where the MD becomes fairly large and missile avoidance is successful. Among them, typical fighter air-combat maneuvers are found, such as downward split-S, horizontal-S, linear acceleration, and high-g barrel roll. Some examples of these cases are given next.

Figures 6 through 9 show the missile and aircraft trajectories, histories of aircraft angle of attack α, and roll angle ϕ. Figure 6 illustrates a typical split-S (a kind of sustained maximum g turn). After the 1-s command ϕ (= 0 deg), the aircraft quickly rolls to -180 deg with maximum α. The resulting MD is 30.4 m. Figure 7 shows a typical horizontal-S, where the aircraft first quickly rolls to more than 180 deg, then reverses roll directions. In the maneuver, α is maintained at almost its maximum value. Figure 8 depicts linear acceleration, where the aircraft first takes maximum α, but after 6 s, then takes minimum α (the minimum α value is introduced in order to avoid the singular point at $\alpha = 0$) and accelerates its velocity. At the sustainer phase (maintaining the missile velocity with a sustainer), this type of aircraft maneuver becomes ineffective against a missile. These aircraft maneuvers are discussed in Ref. 8, where the split-S and horizontal-S appear as optimal maneuvers. Figure 9 shows the case of tail-chase geometry, where the aircraft avoids a missile by HGB (high-g barrel roll). HGB has not been verified as optimal, but its effectiveness is well illustrated in Refs. 5 and 9. It seems that when there is an initial heading error, this HGB tends to appear often. Many of the aircraft maneuvers near $\eta = \pm 90$ deg in Fig. 5 are of this type. Another tendency of successful aircraft maneuvers is that they end up as downward evasion. Our previous study[7] showed that a downward evasive maneuver is more efficient than an upward one. In fact, in a downward maneuver the aircraft pilot makes the best use of gravity acceleration, and as the altitude increases, the importance of gravity increases. Although the role of gravity is not a major one in the altitude selected, its effect, however, is revealed in the simulation results.

Conclusions

A pursuit-evasion game between a realistic missile and an aircraft is studied by carrying out massive simulations in the parameter space of initial geometries and guidance law parameters. A guidance law based on augmented proportional navigation, which employs the opponent's acceleration information, shows far superior performance for both vehicles and emphasizes the importance of such information. Since the basic idea of the aircraft evasive guidance law is to constantly produce the LOS rate, a strategy for rotating the relative LOS vector is introduced in this paper for the first time. The results indicate that this strategy is quite effective, particularly at a rotational angle near ± 90 deg, and the aircraft maneuver takes on a pattern like a high-g barrel roll. Among the other cases that appeared successful for the aircraft (producing a large miss distance) are split-S, horizontal-S, and linear acceleration. Since these maneuvers have been obtained in other papers by solving nonlinear two-point boundary-value problems, this fact suggests that the method presented here would be a useful approach in very complicated pursuit-evasion games.

Acknowledgments

The author is indebted to S. Uehara, Director General for Research and Development of the Japan Defense Agency, and T. Ishihara, former fighter pilot and current manager of Mitsubishi Electric Corporation, for giving us useful advice and discussing the contents of this paper.

References

[1]Hillberg, C., and Järmark, B., "Pursuit-Evasion Between Two Realistic Aircraft," *Journal of Guidance, Control, and Dynamics,* Vol. 7, No. 6, 1984, pp. 690-694.

[2]Menon, P. K. A., "Short-Range Nonlinear Feedback Strategies for Aircraft Pursuit-Evasion," *Journal of Guidance, Control, and Dynamics,* Vol. 12, No. 1, 1989, pp. 27-32.

[3]Isaacs, R., *Differential Games,* Wiley, New York, 1965.

[4]Merz, A. W., "The Homicidal Chauffeur," *AIAA Journal,* Vol. 12, No. 3, 1974, pp. 259-260.

[5]Imado, F., and Miwa, S., "Fighter Evasive Boundaries Against Missiles," *Computer Mathematics with Applications,* Vol. 18, No. 1-3, 1989, pp. 1-14.

[6]Zhou, H., and Kumar, K. S. P., "A Current Statistical Model and Adaptive Algorithm for Estimating Maneuvering Targets," *Journal of Guidance, Control, and Dynamics,* Vol. 7, No. 5, 1984, pp. 596-602.

[7]Imado, F., and Miwa, S., "The Optimal Evasive Maneuver of a Fighter Against Proportional Navigation Missiles," AIAA Paper 83-2139, Aug. 1983.

[8]Imado, F., and Miwa, S., "Fighter Evasive Maneuvers Against Proportional Navigation Missile," *Journal of Aircraft,* Vol. 23, No. 11, 1986, pp. 825-830.

[9]Imado, F., and Miwa, S., "Three Dimensional Study of Evasive Maneuvers of a Fighter Against a Missile," AIAA Paper 86-2038, Aug. 1986.